

This is an Accepted Manuscript version of the following article, accepted for publication in:

A. Arrizabalaga *et al.*, "Integration of Silicon Carbide devices to increase the AEP (Annual Energy Production) in a PM based wind generation system," *2020 IEEE 11th International Symposium on Power Electronics for Distributed Generation Systems (PEDG)*, Dubrovnik, Croatia, 2020, pp. 482-486.

DOI: <https://doi.org/10.1109/PEDG48541.2020.9244477>

© 2020 IEEE. Personal use of this material is permitted. Permission from IEEE must be obtained for all other uses, in any current or future media, including reprinting/republishing this material for advertising or promotional purposes, creating new collective works, for resale or redistribution to servers or lists, or reuse of any copyrighted component of this work in other works.

Integration of Silicon Carbide devices to increase the AEP (Annual Energy Production) in a PM based wind generation system

Antxon Arrizabalaga
Mondragon Unibertsitatea
Hernani, Spain
aarizabalaga@mondragon.edu

Mikel Mazuela
Mondragon Unibertsitatea
Hernani, Spain
mmazuela@mondragon.edu

Aitor Idarreta
Mondragon Unibertsitatea
Hernani, Spain
aitor.idarreta@alumni.mondragon.edu

Unai Iraola
Mondragon Unibertsitatea
Hernani, Spain
uiraola@mondragon.edu

Iosu Aizpuru
Mondragon Unibertsitatea
Hernani, Spain
iaizpuru@mondragon.edu

José Luis Rodríguez
SGRE Innovation & Technology S.L
Sarriguren Spain
jose.l.rodriguez@siemensgamesa.com

Daniel Labiano Andueza
SGRE Innovation & Technology S.L
Sarriguren Spain
daniel.labiano.ext@siemensgamesa.com

İbrahim Alişar
Siemens Gamesa Renewable Enerji
A.S.
Izmir, Turkey
ibrahim.alisar@siemensgamesa.com

Abstract—A radical energetic change is needed nowadays and enhancing renewable energies should play a main role. For its superior performance and lower losses, SiC devices are identified as a potential technology to improve wind energy generation systems AEP. A 2 MW PM generator based WGS (Wind Generation System) is modeled, and Si IGBT, hybrid and full SiC MOSFET devices are tested in different operation points, as well as different locations. Higher efficiency in the converter based on SiC MOSFETs is observed in all the operation points. This leads to an increment in AEP, mostly in regions with lower average annual wind speeds, making them more interesting for wind energy. The work is replicable tuning the simulation models to obtain precise results for an exact WGS.

Keywords—Wind energy, Modeling, FC, PM, SiC, AEP.

I. INTRODUCTION

The actual society is seeking a radical energetic revolution due to critical climate change [1]. The United Nations 2030 Agenda will try to “Ensure access to affordable, reliable, sustainable and modern energy for all” [2]. In addition, one of the Horizon Europe research initiative missions is “Adaptation to climate change including societal transformation”[3]. For this reason, looking for efficiency improvement in power electronics related to renewable energy

generation, as well as increasing the annual energy production (AEP) of such energy generation systems is considered a key contribution to the actual society.

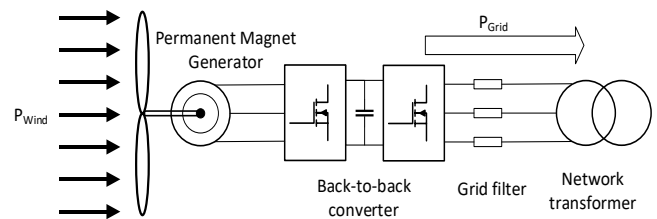


Fig. 1. WGS with PM generator and FC configuration.

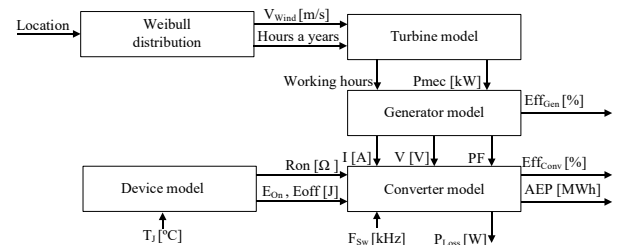


Fig. 2. WGS model diagram.

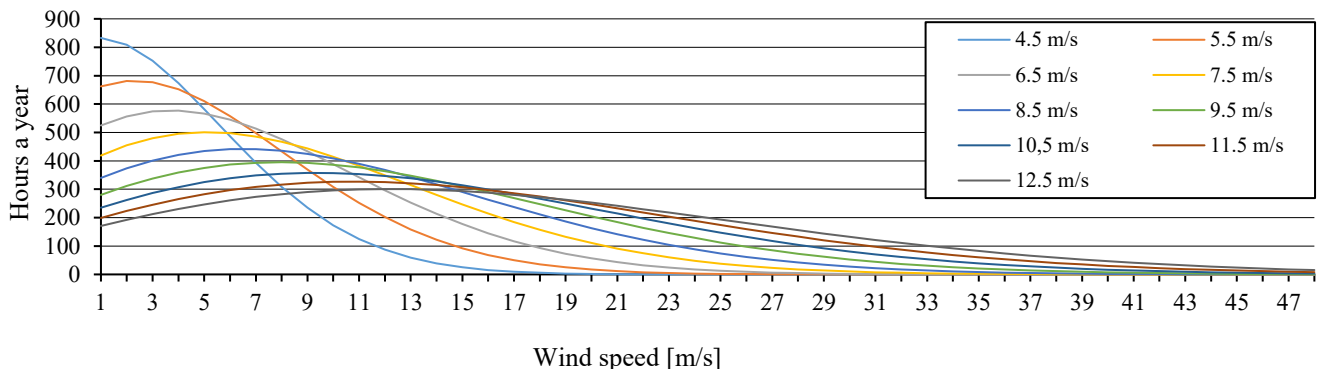


Fig. 3. Hours a year for different average annual wind speed locations.

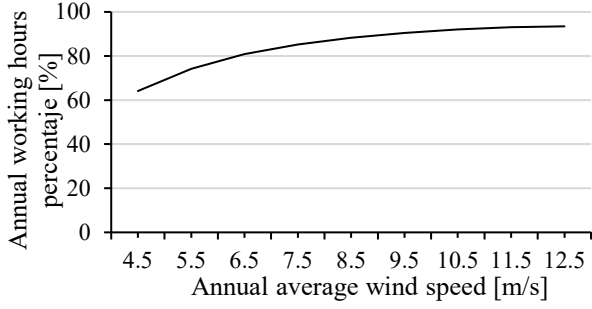


Fig. 4. Annual working hours percentage for different average annual wind speeds.

SiC semiconductors can be used to enhance wind energy performance [4]–[11], reducing the volume of the passive components, the cooling system requirements, and increasing the converters efficiency, in full converter (FC) configuration. However, the effect of that efficiency improvement is having on the AEP in regions with different average annual wind speeds has not been evaluated. This paper analyses the way SiC semiconductors (hybrid, Si IGBT and SiC diode, and full SiC MOSFET) affect the AEP of wind generation systems (WGS), with permanent magnet (PM) generator and FC configuration, Fig. 1. The analysis is carried out by simulation, connecting models of every component of the system, Fig. 2, considering different locations, by using Weibull distributions with form factor 2 [12]–[16], providing the wind speed and the annual hours at a certain wind speed.

II. PM BASED WIND GENERATION SYSTEM MODELLING

A 2 MW WGS with PM generator and FC configuration have been modeled. In this section, every model used for the whole simulation, Fig. 2, is explained in detail.

A. Wind profile model based on Weibull distribution

A Weibull distribution with form factor 2 is used to determine the wind profile of a location, depending on the average annual wind speed. Thus, wind speed and the hours at every wind speed are provided to the wind turbine model. This Weibull distribution can be seen in Fig. 3.

B. Wind turbine model

This model is an aerodynamic representation, based on look up tables from manufacturers. The example is percentage for the selected turbine, depending on the annual

presented in [17]. Mechanical power and working hours are estimated for different locations. The turbine can work with average wind speed of the location is shown in Fig. 4. This wind speeds from 3 to 25 m/s. The working hours shows that over 80 % of the hours can be used to generate energy in locations with average wind speeds superior to 6.5 m/s.

C. PM generator model

The mechanical power is converted to electrical power by the generator model, using analytic equations in [4]. It provides voltage, current and power factor to the converter model for every mechanical power. Electrical input variables are generated for the converter model.

D. Device model

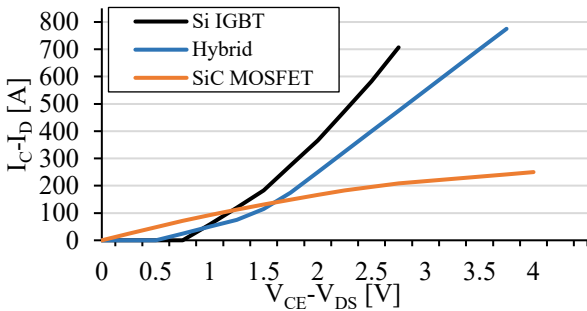
Datasheet information is used to represent the devices performance, as done in [11]. A comparison of the conduction and switching characteristics of the selected modules is shown in Fig. 5 for every semiconductor technology. The silicon IGBTs used for the generator side and grid side characteristics are similar, so considered equal in this study.

Fig. 5 (a) shows the conduction characteristics of every semiconductor technology. As it can be observed, the SiC device performs better than Si devices in low current. This characteristic is achieved due to the resistive behavior of the SiC MOSFET, while Si IGBTs suffer a direct voltage drop in conduction. Fig. 5 (b) shows switching energies for every current. It can be seen that SiC MOSFETs require lower energies than Si IGBTs, making them more efficient at high switching frequencies. Switching and conduction characteristics are provided to the converter model considering the effect of the junction temperature.

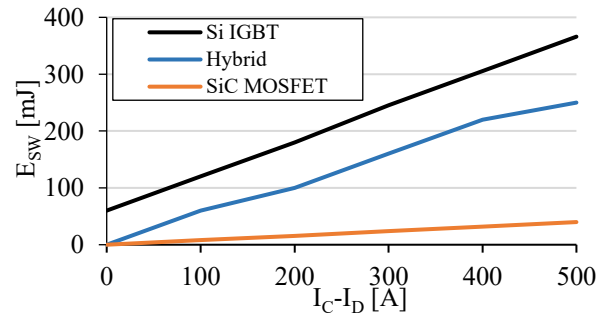
Selected semiconductors can be seen in TABLE. I. In the Si converter, different modules are selected for generator and grid side, for design optimization.

E. Converter model

Analytical equations presented in [18] are used to describe the 2L converters performance in every operation point (1)–(6). The device model provides the required semiconductor data, and the current and voltage waveforms are taken from the generator model. The converter model calculates conduction and switching losses. The efficiency of the converter in every operation point, together with the AEP of the WGS are calculated for the three semiconductors technologies as well as different locations.



(a)



(b)

Fig. 5. Device characteristics comparison, (a) conduction, (b) switching.

TABLE. I. Devices Selected for the WGS

Technology and part number	Rated voltage [V]	Rated current [A]	Configuration generator side	Configuration grid side
Si IGBT: SKiiP 2414 GB17E4-4DUW V2	1700	2400	2 in parallel	/
Si IGBT: SKiiP 3614 GB17E4-6DUW V2	1700	3600	/	1 module
Hybrid: 2MSI400VAE-170-53	1700	400	10 in parallel	7 in parallel
SiC MOSFET: CAS300M17BM2	1700	225	17 in parallel	12 in parallel

The generic expression of conduction losses are shown in (1) [18].

$$P_{Cond} = V_{th} \cdot I_{AV} + R_{ON} \cdot I_{RMS}^2 \quad (1)$$

Being (2) the resulting expression of a MOSFET, (3) for an IGBT and (4) In the case of a diode. ma is the modulation index (5). The parameters for each semiconductor are introduced in every operation point. The V_{th} factor present in the IGBT and diode equation represents the direct voltage drop presented in Fig. 5 (a), and is zero in the case of SiC MOSFETs.

$$P_{Cond_MOSFET} = \frac{1}{2} \cdot \left(R_{ON} \cdot \frac{I_{max}^2}{4} \right) + ma \cdot \cos(\varphi) \cdot \left(\frac{R_{ON} \cdot I_{max}^2}{3 \cdot \pi} \right) \quad (2)$$

$$P_{Cond_IGBT} = \frac{1}{2} \cdot \left(V_{th} \cdot \frac{I_{max}}{\pi} + R_{ON} \cdot \frac{I_{max}^2}{4} \right) + ma \cdot \cos(\varphi) \cdot \left(V_{th} \cdot \frac{I_{max}}{8} + \frac{R_{ON} \cdot I_{max}^2}{3 \cdot \pi} \right) \quad (3)$$

$$P_{Cond_DIODE} = \frac{1}{2} \cdot \left(V_{th} \cdot \frac{I_{max}}{\pi} + R_{ON} \cdot \frac{I_{max}^2}{4} \right) - ma \cdot \cos(\varphi) \cdot \left(V_{th} \cdot \frac{I_{max}}{8} + \frac{R_{ON} \cdot I_{max}^2}{3 \cdot \pi} \right) \quad (4)$$

$$ma = \frac{V_{ac}}{V_{dc}/2} \quad (5)$$

Switching losses are calculated with (6). Parameters a , b and c are obtained for each semiconductor using curve fitting technique from the curves presented in Fig. 5 (b).

$$P_{Sw} = f_{sw} \cdot \frac{V_{bus}}{V_{100FIT}} \cdot \left(\frac{a}{2} + \frac{b \cdot I_{max}}{\pi} + \frac{c \cdot I_{max}^2}{4} \right) \quad (6)$$

III. SIMULATION AND DISCUSSION

In this section, the simulations that have been performed are explained, and the results of those simulations are shown. In addition, the real life application of those results as well as their impact in the actual and future society challenges are studied.

In the first simulation, the efficiency of the converter for every operation point and semiconductor technology is calculated. Next, AEP is calculated for different locations and semiconductor technology. Then, the increment on the AEP is computed depending on the semiconductor and the location.

A. Impact on the converters efficiency

The efficiency of the three converters has been calculated by the converter model, and shown in Fig. 6. SiC MOSFETs based converter has better efficiency in every wind speed, even if the efficiency difference is greater at

low wind speeds. This is due to the conduction characteristics of Si IGBTs and SiC MOSFETs, mentioned previously. The forward voltage drop present in the IGBTs does not penalize SiC MOSFETs, which have a resistive response in every operation point. This effect is attenuated when wind speeds increases, increasing also the current in the converter.

At nominal wind speed (12.5 m/s), the difference between efficiencies is fixed. This is due to the fact that no more than nominal power can be generated by the wind turbine. In this point, pitch-angle control is applied to keep the turbine in MPP (Maximum Power Point), delivering also the maximum current to the converter. This working point is kept until cut-off wind speed is reached at 25 m/s.

B. Impact on the AEP

In Fig. 7, the AEP gain percentage with SiC based semiconductors respect to the actually used Si IGBTs is shown. It can be seen 1.65 % more AEP is gained in regions with 9.5 m/s annual average wind speed using SiC MOSFETs, and 0.8 % with hybrid technology. However, it is observed that the lower the annual average wind speed of the region is, the bigger the impact of SiC based semiconductors is. An increment as high as 2.5 % is achieved in locations with average annual wind speeds of 7.5 with SiC MOSFETs, while 1.22 % is achieved with Hybrid semiconductors.

Even if it must be said that locations with average wind speed around 9.5 m/s are considered potentially interesting for wind generation [19], an increment as high as the 2.5 % on the annual energy production could make new locations with lower average annual wind speed also interesting for wind energy.

C. Application of the results

Fig. 8 shows the AEP in regions with different average annual wind speeds, depending on the semiconductor technology used in the converter. As expected, the higher the average annual wind speed is, the greater the AEP is for every technology, being the greatest for SiC MOSFETs. In regions with potential for wind energy generation, (7.5-9.5 m/s) [19], the evolution of AEP can be very well approximated to first order equations for SiC MOSFETs, hybrid devices and Si IGBTs, Fig. 8. Computing the first order equations of the different technologies, it can be calculated that same AEP can be obtained in locations with around 0.065 m/s less average annual wind speed with SiC, compared to the actually used Si technology. This opens up the possibility to consider new locations for wind energy generation, making this sustainable and renewable energy source available to more communities.

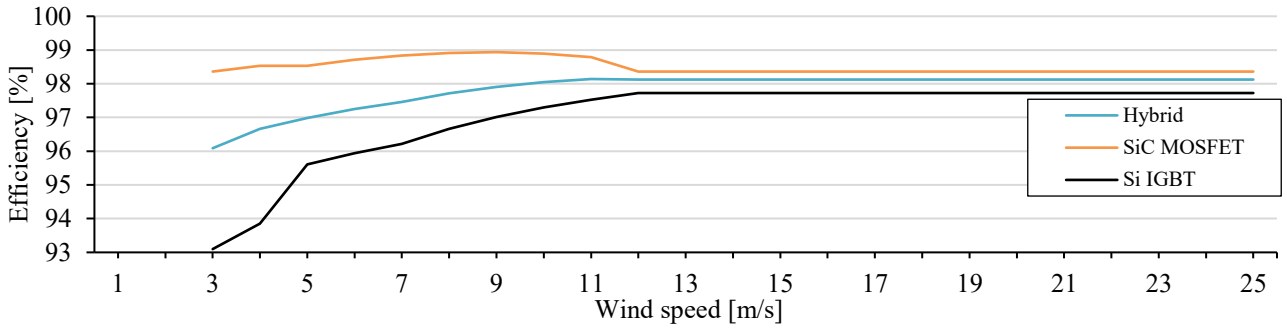


Fig. 6. Efficiency of the converter at different wind speeds and the three different semiconductors.

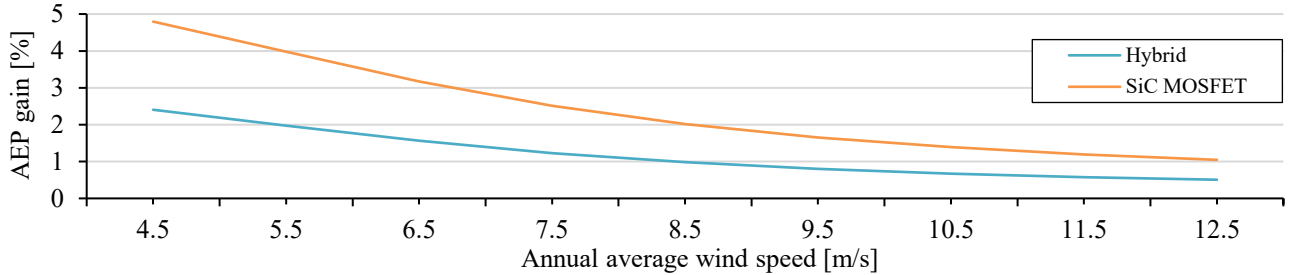


Fig. 7. AEP gain percentage depending on the average annual wind speed of the location for the three different semiconductors, using as reference the actually used Si IGBTs.

On the other hand, it is observed that more energy can be generated with SiC MOSFETs in the same location without any CO₂ emission. If the gained energy in a region with average annual wind speed of 9.5 m/s was generated with coal, 12238 Kg CO₂ would have been emitted in a year [20]. This is equivalent to 94138 Km of driving with a car meeting the 2015 emission goal in EU [21]. All the calculations refer to a single wind turbine, being the results even more relevant in a whole wind farm. The integration of SiC semiconductors in WGS can be a key action to tackle the actual and future challenges of the society.

IV. CONCLUSION

This work has identified two contributions of SiC devices in PM based WGS: First, the efficiency improvement in the converter with SiC MOSFETs, shown in Fig. 6, leads to less cooling requirements. In some cases, this reduction could cause the possibility to move from

water cooled modules to air cooled systems. This action would mean the saving of all the hydraulic circuit, as well as replacing the consumption of the pump for the lower consumption of a fan. Secondly, the efficiency improvement generates an increment on AEP, Fig. 7. This means more energy generated in a sustainable way, saving the hazardous effects of conventional energy generation plants. In addition, this increased capability to generate energy makes new regions interesting for the wind energy generation, Fig. 8. All the numbers and calculations carried out in this paper are a generalist approach and without considering auxiliary power losses. The work is replicable in a certain location, with specifically tuned Weibull wind distribution, wind turbine, generator and device models, with the selected technology parameters, obtaining precise results for an exact WGS.

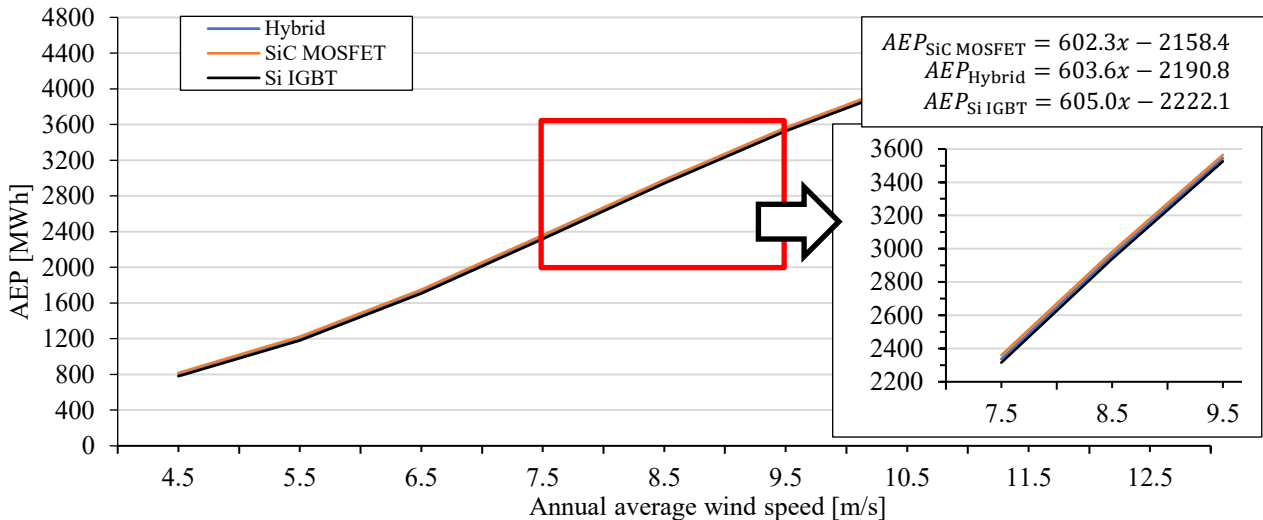


Fig. 8. AEP depending on the average annual wind speed of the location for the three selected semiconductors. Linearization in the regions with wind energy generation potential included.

REFERENCES

- [1] "2019 Was the Second-Hottest Year Ever, Closing Out the Warmest Decade - The New York Times." [Online]. Available: <https://www.nytimes.com/interactive/2020/01/15/climate/hottest-year-2019.html>. [Accessed: 17-Jan-2020].
- [2] "Transforming our world: the 2030 Agenda for Sustainable Development .. Sustainable Development Knowledge Platform." [Online]. Available: <https://sustainabledevelopment.un.org/post2015/transformingourworld>. [Accessed: 09-Jan-2020].
- [3] "Mission area: Adaptation to climate change including societal transformation | European Commission." [Online]. Available: https://ec.europa.eu/info/horizon-europe-next-research-and-innovation-framework-programme/mission-area-adaptation-climate-change-including-societal-transformation_en. [Accessed: 09-Jan-2020].
- [4] H. Zhang and L. M. Tolbert, "SiC's Potential Impact on the Design of Wind Generation System," 2008.
- [5] I. Kortazar, I. Larrazabal, and P. Friedrichs, "Analysis of hybrid modules with Silicon Carbide diodes, comparison with full silicon devices and the impact in Wind applications," in 2016 18th European Conference on Power Electronics and Applications, EPE 2016 ECCE Europe, 2016.
- [6] W. L. Erdman, D. Grider, and E. Vanbrunt, "4500 volt Si/SiC hybrid module qualification for modern megawatt scale wind energy inverters," in 2nd IEEE Workshop on Wide Bandgap Power Devices and Applications, WIPDA 2014, 2014, pp. 1–6.
- [7] A. Hussein and A. Castellazzi, "Variable frequency control and filter design for optimum energy extraction from a SiC wind inverter," in 2018 International Power Electronics Conference, IPEC-Niigata - ECCE Asia 2018, 2018, pp. 2932–2937.
- [8] R. Dey and S. Nath, "Replacing silicon IGBTs with SiC IGBTs in medium voltage wind energy conversion systems," in India International Conference on Power Electronics, IICPE, 2017, vol. 2016-Novem.
- [9] A. Hussein and A. Castellazzi, "Comprehensive design optimization of a wind power converter using SiC technology," in 6th IEEE International Conference on Smart Grid, icSmartGrids 2018, 2019, pp. 34–38.
- [10] A. Castellazzi, E. Gurpinar, Z. Wang, A. S. Hussein, and P. G. Fernandez, "Impact of wide-bandgap technology on renewable energy and smart-grid power conversion applications including storage," *Energies*, vol. 12, no. 23, pp. 1–14, 2019.
- [11] H. Zhang and L. M. Tolbert, "Efficiency Impact of Silicon Carbide Power Electronics for Modern Wind Turbine Full Scale Frequency Converter," *IEEE Trans. Ind. Electron.*, vol. 58, no. 1, 2011.
- [12] L. Van Der Auwera, F. De Meyer, and L. M. Malet, "The use of the Weibull three-parameter model for estimating mean wind power densities," *Journal of Applied Meteorology*, vol. 19, no. 7, pp. 819–825, 1980.
- [13] A. Sarkar, G. Gugliani, and S. Deep, "Weibull model for wind speed data analysis of different locations in India," *KSCE J. Civ. Eng.*, vol. 21, no. 7, pp. 2764–2776, 2017.
- [14] A. N. Celik, "A statistical analysis of wind power density based on the Weibull and Rayleigh models at the southern region of Turkey," *Renew. Energy*, vol. 29, no. 4, pp. 593–604, 2004.
- [15] A. S. S. Dorvlo, "Estimating wind speed distribution," *Energy Convers. Manag.*, vol. 43, no. 17, pp. 2311–2318, 2002.
- [16] E. Gómez-Lázaro et al., "Probability density function characterization for aggregated large-scalewind power based on Weibull mixtures," *Energies*, vol. 9, no. 2, pp. 1–15, 2016.
- [17] G. Abad, J. López, M. A. Rodríguez, L. Marroyo, and G. Iwanski, *Doubly Fed Induction Machine*. 2011.
- [18] B. Ozpineci, L. M. Tolbert, S. K. Islam, and M. Hasanuzzaman, "Effects of silicon carbide (SiC) power devices on HEV PWM inverter losses," *IECON Proc. (Industrial Electron. Conf.)*, vol. 2, no. C, pp. 1061–1066, 2001.
- [19] H. Cetinay, F. A. Kuipers, and A. N. Guven, "Optimal siting and sizing of wind farms," *Renew. Energy*, vol. 101, pp. 51–58, 2017.
- [20] "Carbon Dioxide Emission Factors for Coal." [Online]. Available: https://www.eia.gov/coal/production/quarterly/co2_article/co2.html. [Accessed: 09-Jan-2020].
- [21] "Reducing CO2 emissions from passenger cars | Climate Action." [Online]. Available: https://ec.europa.eu/clima/policies/transport/vehicles/cars_en. [Accessed: 09-Jan-2020].